

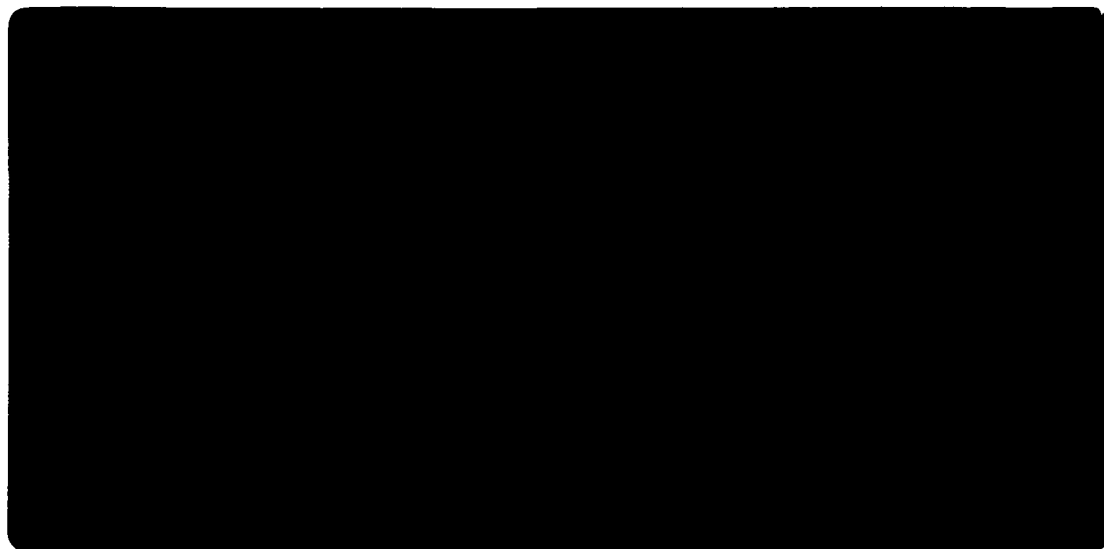


---

*Institute of Paper Science and Technology*  
*Atlanta, Georgia*

---

**IPST TECHNICAL PAPER SERIES**



**NUMBER 469**

**PREDICTION OF PAPER COLOR:  
A PROCESS SIMULATION APPROACH**

**G.L. JONES, M. CHATURVEDI, AND R. ARAVAMUTHAN**

**MARCH 1993**

# Prediction of Paper Color: A Process Simulation Approach

G.L. Jones, M. Chaturvedi, and R. Aravamathan

Submitted to  
Oxford Fundamental Research Symposium  
September 1993  
Oxford, England

Copyright© 1993 by the Institute of Paper Science and Technology

For Members Only

## NOTICE AND DISCLAIMER

The Institute of Paper Science and Technology (IPST) has provided a high standard of professional service and has put forth its best efforts within the time and funds available for this project. The information and conclusions are advisory and are intended only for internal use by any company who may receive this report. Each company must decide for itself the best approach to solving any problems it may have and how, or whether, this reported information should be considered in its approach.

IPST does not recommend particular products, procedures, materials, or service. These are included only in the interest of completeness within a laboratory context and budgetary constraint. Actual products, procedures, materials, and services used may differ and are peculiar to the operations of each company.

In no event shall IPST or its employees and agents have any obligation or liability for damages including, but not limited to, consequential damages arising out of or in connection with any company's use of or inability to use the reported information. IPST provides no warranty or guaranty of results.

**PREDICTION OF PAPER COLOR:  
A PROCESS SIMULATION APPROACH**

**Gary L. Jones  
Institute of Paper Science and Technology  
Atlanta, Georgia USA**

**Mayank Chaturvedi  
Union Camp Corporation  
Franklin, Virginia USA**

**Raja Aravamuthan  
Western Michigan University  
Kalamazoo, Michigan USA**

## TABLE OF CONTENTS

ABSTRACT	1
INTRODUCTION	2
OBJECTIVES	3
THEORETICAL BACKGROUND	3
Color and Its Measurement	3
The CIE L*a*b* Color Scale	4
Measurement of Color Difference	6
Measuring Instruments	6
Reflectance of Paper	7
Light Absorption and Scattering	7
Kubelka-Munk Theory and the Color Prediction of Paper	7
Dye Characteristics	9
Dyeing Practice	10
Effects of Dyes on the Optical Properties of Paper	10
Performance Attributes and End-Use Performance Simulation	10
EXPERIMENTAL	11
DATA ANALYSIS AND MODEL DEVELOPMENT	11
Substrate Reflectance	12
Color Simulation	13
Dye Mixing	14
Optical Property Models	14
Dye K/S Data	15
Model Tuning	15
MODEL VALIDATION	16
Reflectance of Calibration Paper	16
Color of Calibration Paper	18
Effect of Illuminant and Observer Angle	19
Effect of Dye Loading on Color Difference	21
Model Validation - Validation Papers	22
Color Change	24
Lab Values for the Validation Papers	25
Tinted Sheets	27
CONCLUSIONS AND RECOMMENDATIONS	29
REFERENCES	30

## LIST OF TABLES

Table 1 Model Parameters for Substrate Reflectance	12
Table 2 Dye Mixture Combinations for Saturated Validation Papers	29
Table 3 Dye Mixture Combinations for Tinted Papers	30

## LIST OF FIGURES

Figure 1 MAPPS Flow Sheet for Property Model Validation	13
Figure 2 Effect of Pure Dyes on Reflectance- Calibration Handsheets	17
Figure 3 L*a*b* Values for Calibration Handsheets- 2 Degrees C Illuminant	18
Figure 4 Effect of Observer Angle and Illuminant on Color Change - Calibration Handsheets	19
Figure 5 Effect of Observer Angle and Illuminant on Color Change - Calibration Handsheets Measured and Predicted Values	20
Figure 6 Effect of Dye Loading on Color Difference - Calibration Handsheets Red, Blue, and Yellow Dyes	21
Figure 7 Effect of Dye Mixtures on Reflectance of Machine Paper	22
Figure 8 Effect of Dye Mixtures on L*a*b* Values - Machine Papers Red, Blue, and Yellow Dyes	23
Figure 9 Effect of Dye Mixtures on Color Change- Machine Paper, Couch and Validation Handsheets Red, Blue, and Yellow Dyes	25

Figure 10 Effect of Dye Mixtures on L*a*b* Values - Validation Handsheets Red, Blue, and Yellow Dyes	25
Figure 11 Effect of Dye Mixtures on L*a*b* Values - Couch Handsheets Red, Blue, and Yellow Dyes	26
Figure 12 Effect of Tints on Color Change Combined Calibration and Validation Handsheets Mixtures of Red, Blue, and Black Dyes	27
Figure 13 Effect of Tints on L*a*b* Values Combined Calibration and Validation Handsheets Mixtures of Red, Blue, and Black Dyes	28

## ABSTRACT

A simulation system has been developed to predict the optical properties of dyed paper. The system is part of a papermaking process simulation program and is intended for use as part of an on-line color control system to reduce variations in color for dyed paper grades. The system calculates the effects of mixing of multiple primary dyes with fiber streams and the optical characteristics of the base paper. The optical properties predicted by the system include the reflectance at 20 nm intervals over the range of visible wavelengths (400 to 700 nm), CIE L\*a\*b values, and Tappi Brightness and opacity. The models were developed from handsheet data and validated with both handsheet and pilot paper machine data. Predictions are valid for a wide range of dye saturations (base sheet, tints to light saturated) and combinations of two observer angles (2 and 10 degree standard observers) and two illuminants (C and D65) and for combinations of red, blue, and black dyes at light loadings and red, yellow, and blue dyes for light to heavy loadings.

This paper describes color theory, modeling, and experimental methodology, and compares the results of the reflectance and CIE L\*a\*b\* models with data for both pure dyes and mixtures of dyes applied to several different types of pilot papers.

## INTRODUCTION

Color uniformity is a particularly important quality characteristic for fine paper manufacturers. Paper is colored by the addition of various dyes to paper stock in the stock preparation system just before sheet forming. Traditionally, dyes have been added in the stock blending chest, and sufficient mixing time is required for the uniform distribution and fixing of the dyes on the fibers. So-called direct dyes have a strong affinity for cellulose, making it possible to add them directly to the furnish. The development of liquid anionic and cationic direct dyes made possible the continuous addition of dyes in the stock.

The introduction of on-line spectrophotometers and microprocessor-based control systems has led to the closed loop control of color to any desired shade. However, on-line measurements are made in the wet state and, therefore, require adjustment to control final dry state color. Thus, it would be useful to have a model to predict color in the dry state as a way of improving control of final sheet color.

The coloring of paper is very sensitive to changing process conditions during paper making. Variations in the flow and retention of the dyes affect the final sheet color, its quality and uniformity. Considering the complex nature of color and its interactions with papermaking variables, a reliable simulation system would certainly be preferable to time-consuming and costly pilot-plant trials for design and troubleshooting. Color simulation can provide useful insights into effects of changing process conditions on color variations. Simulation can also be used to guide and interpret pilot experiments. In combination with experimental data, a process simulation model can be used to determine process parameters which may be difficult or impossible to measure directly. Process simulation makes it possible to perform 'what-if' analysis by quantifying the effects of changing process variables.

The development of a color simulation model is made easier by starting with an already available simulation package such as MAPPS (Modular Analysis of Pulp and Paper Systems). The unique features of MAPPS, particularly the Performance Attribute (PAT) modeling feature, provide the framework necessary to model dye mixing and color matching. The PAT system is currently used to simulate a wide variety of end-use performance properties (such as compressive, elastic, tensile, and optical) of various paper grades. In a later section, the connection between the PAT system and the color prediction program will be described in more detail.

## OBJECTIVES

The specific objectives of this work were to measure the reflectance and color of both handsheets and machine papers under representative dyeing conditions and to develop and validate a modeling system to predict color and other optical properties from first principles. It was also desirable that the simulation system predict reflectance and CIE Lab values for combinations of 2 and 10 degree observer angles and C and D65 illuminants over a wide range of dye loadings and for a variety of colorant classes. The optical property system must also predict Tappi Brightness and Opacity at 457 nm and Tappi printing opacity at 572 nm.

## THEORETICAL BACKGROUND

### Color and Its Measurement

Color is a **psychological** response to a physical stimulus. The eye and central nervous system "see" color based on three components: the light source, the object, and the human observer (2). The light source defines an illumination condition which affects the way we see color. For example, color is perceived differently in natural light from artificial light. The International Commission on Illumination (Commission Internationale de L'Eclairage) or CIE has recommended various illuminants as light sources (3). These can be divided into tungsten light and artificial daylight.

The CIE established two different standard illuminants (B and C) to represent daylight. However, B and C have too little relative spectral power in the UV region which creates problems with fluorescent colors. D65 was designed to represent average daylight throughout the visible spectrum and into the UV region as far as 300 nm(3).

The appearance attributes of an object are related to the ways in which the object modifies the light that strikes it. Interactions of light with a object result in the specular reflection (related to gloss), scattering within the object (associated with diffuse reflection and diffuse transmission), absorption within the material (associated with color), and rectilinear transmission directly through the object (associated with clarity).

The perception of color is the result of how the human eye interprets the light reaching it from the object. In 1931, the CIE developed a standard observer to complete the description of the response to color of the normal human eye. The observer is defined in terms of color matching functions  $x(\lambda)$ ,  $y(\lambda)$ ,  $z(\lambda)$  (4). The 1931, CIE standard observer was based on a 2 degree field of view which was not sensitive to shortwave violet as observers tend to do when grading products with their eyes. In 1960, the CIE proposed a 10 degree standard observer which provides better correlation with commercial judgements (4). Standard observer and illuminant data are used to quantify color in terms or so-called **tristimulus values** of the color object.

The standard coordinates of the 1931 CIE system, the tristimulus values X, Y, and Z, are calculated from the spectral reflectance factors  $R(\lambda)$  over the visible range of 400-700 nm. These factors are the reflectance at each wavelength from an object as a decimal fraction of that reflected by a perfect reflecting diffuser (e.g., Magnesium Oxide or Barium Sulfate) identically illuminated. At each wavelength interval,  $R(\lambda)$  is multiplied by  $S(\lambda)$ , the relative spectral power distribution of the illuminant, and by each of the three color matching functions  $x(\lambda)$ ,  $y(\lambda)$ , and  $z(\lambda)$  and summed over a wavelength range.

$$\begin{aligned} X &= k \sum R(\lambda)S(\lambda)\bar{x}(\lambda) \\ Y &= k \sum R(\lambda)S(\lambda)\bar{y}(\lambda) \\ Z &= k \sum R(\lambda)S(\lambda)\bar{z}(\lambda) \end{aligned} \tag{1}$$

The scaling factor  $k$  is defined as

$$k = \frac{100}{\sum S(\lambda)\bar{y}(\lambda)} \tag{2}$$

which means that Y of the perfect reflecting diffuser and therefore of the illuminant used in the calculation is always 100. The X, Y, and Z values for the illuminants C and D65 at a 2 degree and 10 degree field of view may be found in Ref 1.

The CIE tristimulus values X, Y, and Z have limited use for specifying colors. The Y value correlates with lightness, but X and Z by themselves do not correlate with visual attributes such as hue, saturation, depth, vividness, redness-greenness, and yellowness-blueness (5). Over the years many color scales which correlate well with visual attributes have been developed, but only the CIE  $L^*a^*b^*$  color scale has gained popularity among practitioners.

### The CIE $L^*a^*b^*$ Color Scale

To achieve a uniformity of practice, the CIE in 1976 officially recommended an approximately uniform color space standard known as the CIE 1976  $L^*a^*b^*$  space (6).

The quantities are defined in terms of X, Y, and Z as follows,

$$\begin{aligned}
 L^* &= 116 \left[ \frac{Y}{Y_n} \right]^{1/3} - 16 && \text{for } \frac{Y}{Y_n} > 0.008856 \\
 L^* &= 903.3 \frac{Y}{Y_n} && \text{for } \frac{Y}{Y_n} \leq 0.008856
 \end{aligned} \tag{3}$$

$$a^* = 500 \left[ f \left( \frac{X}{X_n} \right) - f \left( \frac{Y}{Y_n} \right) \right] \tag{4}$$

$$b^* = 200 \left[ f \left( \frac{Y}{Y_n} \right) - f \left( \frac{Z}{Z_n} \right) \right] \tag{5}$$

where

$$\begin{aligned}
 f \left( \frac{X}{X_n} \right) &= \left( \frac{X}{X_n} \right)^{1/3} && \text{for } \frac{X}{X_n} > 0.008856 \\
 f \left( \frac{X}{X_n} \right) &= 7.787 \left( \frac{X}{X_n} \right) + \frac{16}{116} && \text{for } \frac{X}{X_n} \leq 0.008856
 \end{aligned} \tag{6}$$

and

$$\begin{aligned}
 f \left( \frac{Y}{Y_n} \right) &= \left( \frac{Y}{Y_n} \right)^{1/3} && \text{for } \frac{Y}{Y_n} > 0.008856 \\
 f \left( \frac{Y}{Y_n} \right) &= 7.787 \left( \frac{Y}{Y_n} \right) + \frac{16}{116} && \text{for } \frac{Y}{Y_n} \leq 0.008856
 \end{aligned} \tag{7}$$

$$\begin{aligned}
 f\left(\frac{Z}{Z_n}\right) &= \left(\frac{Z}{Z_n}\right)^{\frac{1}{3}} & \text{for } \frac{Z}{Z_n} > 0.008856 \\
 f\left(\frac{Z}{Z_n}\right) &= 7.787\left(\frac{Z}{Z_n}\right) + \frac{16}{116} & \text{for } \frac{Z}{Z_n} \leq 0.008856
 \end{aligned}
 \tag{8}$$

Subscript "n" designates the reference white. The CIELAB space is used to compare differences between the object colors of the same size and shape, viewed in identical white to midgrey surroundings by an observer. For the illuminants C and D65 at the 2 and 10 degree viewing angles, the values of  $X_n$ ,  $Y_n$ , and  $Z_n$  for the perfect diffuser are given in Ref. 1.

### Measurement of the Color Difference

The color difference between two papers as seen by the eye can be determined using the following color difference equation defined by the CIE in 1976 (7),

$$\Delta C = \sqrt{(\Delta L^*)^2 + (\Delta a^*)^2 + (\Delta b^*)^2}
 \tag{9}$$

where  $\Delta L^*$ ,  $\Delta a^*$ , and  $\Delta b^*$  are the differences in  $L^*$ ,  $a^*$  and  $b^*$  values between two samples, and  $\Delta C$  is the visual color difference between two samples. These differences quantify in a compact form the differences perceived by the eye. For example, the color difference between black and white samples is 100  $\Delta C$  units. The tolerance in commercial color matches is usually less than one  $\Delta C$  unit.  $\Delta C$  could also be defined in terms of the deviations between measured and predicted values of  $L$ ,  $a$ , and  $b$  (Eq. 10 top).  $\Delta C$  could also be defined in terms of deviations from a reference such as the undyed sheet as defined in Eq. 10 (bottom). This definition is used in the following discussion to describe the so-called color change which occurs as various dyes are applied.

$$\begin{aligned}
 \Delta L &= L^*_{meas} - L^*_{pred} \\
 \Delta L &= L^* - L^*_{ref}
 \end{aligned}
 \tag{10}$$

Similar definitions apply to  $a^*$  and  $b^*$ .

### Measuring Instruments

Two types of color measuring instruments commonly used are the colorimeter and the spectrophotometer. With each instrument the sample is illuminated with a standard

source and the reflected light passes through a filter or grating and then enters the detector where the signal is converted into tristimulus values.

## **Reflectance of Paper**

### **Light Absorption and Scattering**

The interaction of light with paper can be explained by the scattering and absorption properties of the paper. The absorption of light, described by an absorption coefficient,  $K$ , is defined as the relative decrease of the flux in a collimated beam of light due to absorption in a differential path length, divided by the differential path length (8,9).

To predict scattering coefficient, both the strength of scattering and the angular distribution of the scattered light are required. The strength of scattering can be described by a linear scattering coefficient, defined as a relative decrease of the flux in a collimated beam of light due to scattering in a differential thickness, divided by the differential path length (8). The angular distribution of light can be described by the angle of deflection of the scattered light from its direction of travel before being scattered. For approximately diffuse radiation, the ratio of scattering coefficient for diffuse light to scattering coefficient for collimated light has a value of 1.0 for highly absorbing and 0.5 for negligibly absorbing materials (9).

Kubelka and Munk developed an approximate theory relating these coefficients to the reflection and transmission in a turbid medium. This theory is approximate because light is assumed to be moving upward and downward only. Multiflux theories have been developed to account for light travel in all directions (10).

### **Kubelka-Munk Theory and the Color Prediction of Paper**

This theory represents the exact solution to a specific problem of absorption and scattering of electromagnetic radiation. The Kubelka-Munk theory rests on a substantial number of assumptions:

1. The colorant layers such as paper consist of optically identical elementary layers
2. The light beam consists of two completely diffuse light fluxes, one proceeding downward through the layer and the other one proceeding upward.
3. Light is not polarized, and both illumination and viewing use a diffuse light source.
4. Object has a plane, parallel surface, and no light losses occur at the edges.
5. The effects of large particles, agglomeration, or orientation of the particles in the layer are neglected.
6. Optical contact is assumed with the next layer.
7. Scattering particles are assumed to be large in comparison to the wavelength of the light but small compared to the thickness of the layer.
8. Reflections from the upper side of the boundary are ignored.

The relationship between  $R_{\infty}$ , the reflectivity of a sample, and the absorption and scattering coefficients,  $K$  and  $S$ , was found by approximate exponential solutions by Kubelka and Munk (11) as

$$\frac{K}{S} = \frac{(1 - R_{\infty})^2}{2R_{\infty}} \quad (11)$$

or in terms of reflectance,

$$R_{\infty} = 1 + \frac{K}{S} - \sqrt{2\frac{K}{S} + \left(\frac{K}{S}\right)^2} \quad (12)$$

The theory is applied to one wavelength of light at a time. The continuous reflectance curve is approximated by taking measurements for sixteen or thirty-two discrete wavelengths (12).

The Kubelka-Munk theory has been extensively used in the paper industry (13). The K-M theory has been applied to determine the mathematical relationship between basis weight, reflectance, contrast ratio, and other optical properties of a paper sheet (14). Given measurements of both  $R_0$  and  $R_{\infty}$ , where  $R_0$  is the reflectance of the single sheet of paper with black backing, the absorption and scattering coefficients  $K$  and  $S$  can be calculated using the following relationship (11).

$$K = \frac{1}{2W} \left[ \frac{1 - R_{\infty}}{1 + R_{\infty}} \right] \ln \left[ \frac{1 - R_0 R_{\infty}}{1 - \frac{R_0}{R_{\infty}}} \right] \quad (13)$$

and

$$S = \frac{1}{2W} \left[ \frac{1}{\frac{1}{R_\infty} - R_\infty} \right] \ln \left[ \frac{1 - R_0 R_\infty}{1 - \frac{R_0}{R_\infty}} \right] \quad (14)$$

where  $W$  is the sheet basis weight.

The K-M theory has been applied to describe the effects of dyeing on the reflectance of the paper (15). It is assumed that dyes do not contribute to the scattering of the sheet and change only the specific absorption coefficient (16). The relationship between dye concentration and K/S ratio is given by the following mixture rule (15).

$$\left( \frac{K}{S} \right)_{mixture} = \sum_{i=1}^n C_i \left( \frac{K}{S} \right)_{dye\ i} + \left( \frac{K}{S} \right)_{substrate} \quad (15)$$

K/S for each dye is defined at concentration,  $C_i$ , based on bone-dry fiber. The substrate refers to the undyed base sheet.

If the absorption coefficient of each dye is known and light scattering is caused only by the substrate, the above equation reduces to the following form (16),

$$\left( \frac{K}{S} \right)_{dyed\ sheet} = \left( \frac{K}{S} \right)_{substrate} + \sum_{i=1}^n C_i K_i \quad (16)$$

where  $K_i$  is the specific absorption coefficient of dye  $i$ , and  $n$  is equal to the total number of dyes used.

Color can be predicted by first predicting the reflectivity of the paper sheet over the range of visible spectrum (400 to 700 nm) at discrete wavelengths. The tristimulus values are then calculated by numerical integration as described earlier.

### Dye Characteristics

The paper industry has used four major colorant classes for dyeing paper to various shades. These are acid dyes, basic dyes, direct dyes, and colored pigments. Basic dyes are primarily used for unbleached grades (17). Acid dyes and pigments are used for special fine papers to provide certain effects such as brightness and light-fastness.

Direct dyes have either an anionic or cationic surface charge and are the most common dyes used in the production of bleached papers because they adsorb on cellulose without the need for mordants, fixatives, or alum.

### **Dyeing Practice**

Dyeing of pulps is dependent on sorption processes, preceded by transport phenomena (mainly diffusion) and frequently accompanied by chemical reactions. The dyeing process can be described by dyeing kinetics (transport and reaction phenomena) and dyeing statics (sorption and desorption processes in the state of equilibrium). The kinetics of dyes is affected by processing conditions such as variation in contact time, temperature, and pH. Direct dyes have direct affinity for fibers and follow the Freundlich Isotherm when applied to cellulose (18). Cationic direct dyes have been shown to be 95% exhausted after about 30 seconds exposure to either bleached sulfite or bleached kraft pulp (19).

### **Effects of Dyes on the Optical Properties of Paper**

The addition of dyes can affect all three important optical properties of paper: color, brightness, and opacity. Each dye has a characteristic absorption or reflectance curve. The shape and reflectance at the point of maximum absorption of light influence optical properties of the paper. The maximum absorption of light varies with the dye structure.

The opacity of paper is measured at 572 NM wavelength as defined by TAPPI standard tests T 425 om-86 and T 519 om-86. The opacifying power of dyes depends on the absorption of light in the wavelength region for which the human eye is most sensitive (approx. 555 NM). The opacifying effectiveness depends on the shade of the dye, depth of the shade, and the width of the absorption area (20). The most effective dyes for providing opacity are black, violets, and blues. The least effective dyes are yellows and oranges.

The brightness of paper is measured at a 457 NM light wavelength as defined by TAPPI T 452 om-87 and T 525 om-86. Except for the fluorescent dyes, colorants decrease brightness. The brightness of paper is least reduced by dyes which show maximum reflectance around 457 NM (20).

### **Performance Attributes and End-use Performance Simulation**

The system to predict paper properties incorporated into MAPPS (Release 3.2 and higher) (21) is called the Performance Attribute or PAT system. Performance attribute simulation modeling has been applied to many areas of papermaking (22,23,24,25,26). An accurate prediction of the brightness and color of a dyed sheet is important for simulation of manufacture of fine papers. Therefore, the objective of this work was to

develop MAPPS modules to simulate dye mixing and optical properties of dyed paper.

## EXPERIMENTAL

The experimental plan consisted of two phases, a model calibration phase and a model validation phase.

In part 1, handsheets were prepared with a series of pure dyes. Two sets of dyes were used to calibrate the model. For the saturated dyeing conditions, the primary color dyes were selected for their color and affinity for cellulose. A red, blue, and yellow dye were selected to cover the entire visible light spectrum. Calibration handsheets were prepared with each single dye at weight fractions of 0 (undyed), 0.5, 1.5, 2.5, 5.0, and  $7.5 \times 10^{-3}$ , respectively. A second set of handsheets was prepared with three different direct dyes (red, blue, and black) at light tint loadings.

In part 2, both handsheets and pilot machine papers were prepared with mixtures of dyes with saturated and tinted shades. Loadings varied from 0 to  $7.5 \times 10^{-3}$  (wt. fraction) for the saturated samples and from 0 to  $0.155 \times 10^{-3}$  (equivalent to 5 oz./ton) for the tinted shades. The dye loading combinations are summarized in Tables 2 and 3.

Two handsheets were prepared for each optical test, and four samples were tested for each dye concentration condition. The nonglossy side of the sample was measured for reflectance. The recorded measurements included the reflectance curve of the sample and CIE  $L^*$ ,  $a^*$ , and  $b^*$  values for illuminants C and D65 for 2 degree and 10 degree observers. Each sample was measured once with a black backing and once with a backing of a thick pad of same sample. This provided reflectance with black backing, i.e.,  $R_b$ , and reflectivity, i.e.,  $R_w$ , measurements for each sample. The CIE  $L^*$ ,  $a^*$ , and  $b^*$  values for each sample were measured with a backing of a thick pad of the same sample. The color of the calibration handsheets varied from light to medium shade.

## DATA ANALYSIS AND MODEL DEVELOPMENT

The average and standard deviation of the reflectivity were calculated at each measured wavelength. Using the data of reflectivity and reflectance with black backing and basis weight of each paper sample, K and S were then determined from Eqs. 13 and 14, respectively. The ratio of K/S was then calculated.

The coefficients of Eq. 16 were determined by linear regression to represent the incremental effect of dye concentration on the K/S value of each paper sample. The K/S of the substrate was subtracted from the K/S of the dyed sample.

## Substrate Reflectance

To predict the reflectance curve of a dyed sheet, it is necessary to specify the reflectance curve of the substrate. This is a function of pulping and bleaching conditions and the wavelength of light. The effects of pulping yield and kappa number are reflected in both light absorption and scattering coefficient, while bleaching influences mainly absorption coefficient. The Performance Attribute system passes the absorption of all components at 457 nm. Scattering at 457 nm is derived from other attributes. Therefore, it is possible to compute K/S at 457 nm (brightness) for any stream containing fibers or other suspended material. Thus, the most convenient way to adjust or compensate for changes in papermaking or pulping conditions is to introduce  $(K/S)_{457}$  as an index to adjust the K/S response. The resulting expression for K/S of the substrate (pulp) is shown in Eq. 17.

$$\left(\frac{K}{S}\right)_{\text{undyed pulp}} = \beta_0 + \beta_1\lambda + \beta_2\left(\frac{K}{S}\right)_{\lambda=457} + \beta_3\lambda^2 + \beta_4\lambda^3 + \beta_5\lambda\left(\frac{K}{S}\right)_{\lambda=457} \quad (17)$$

The coefficients and model fit statistics are shown in Table 1. The high R-squared value indicates the model fit is very good.

PARAMETER	ESTIMATE	PARAMETER	ESTIMATE
$\beta_0$	1.159217185	$\beta_1$	-0.00592605
$\beta_2$	2.811794256	$\beta_3$	$-0.9946 \times 10^{-5}$
$\beta_4$	$0.5 \times 10^{-8}$	$\beta_5$	-0.004223745
R-SQUARED	0.98	DEGREES OF FREEDOM	256

Table 1. Model Parameters for Substrate Reflectance

The above model was developed with known values of K/S (brightness) at 457 nm (approximated by the value at 460 nm) for the calibration handsheets. The model was validated by predicting the reflectance and color of the validation sheets using the MAPPS PAT system.

Using Eqs. 16 and 17,  $R_w$  was predicted at discrete wavelengths from 400 to 700 nm for each of the calibration and validation conditions. The CIE  $L^*a^*b^*$  values are then determined from Eqs. 3 through 8 for the validation conditions. Color error was

predicted from Eq. 9 based on differences between measured and predicted Lab values and relative color change was predicted from Eq. 9 based on differences between measured or predicted Lab values at a given level of dye loading and the undyed values.

### Color Simulation

Two new computer modules were added to the MAPPS system to represent dye mixing and absorption and to compute optical properties. Referring to Figure 1, these were DYEMIX and OPTPROP. Figure 1 is a simplified three-step process flow sheet used to initialize the paper stream and PAT variables (WOOD02 block 1), to mix and adsorb dye (DYEMIX block 2), and to compute optical properties (OPTPROP block 3).

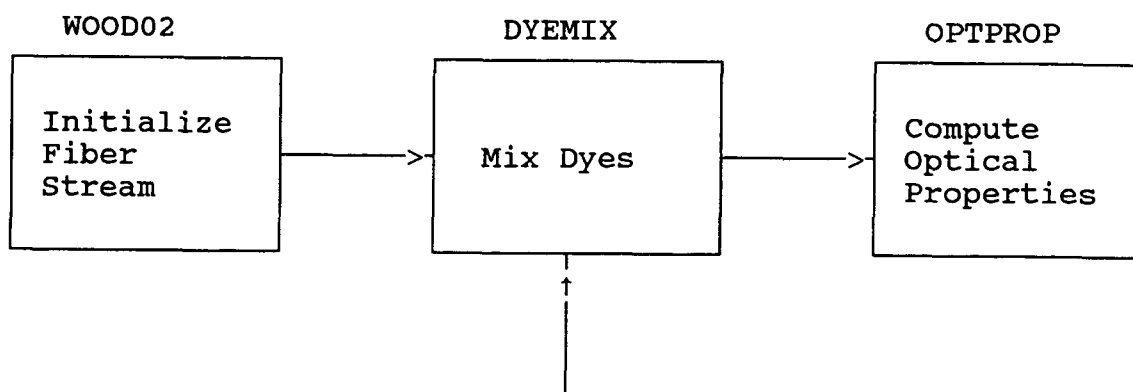


**Figure 1 MAPPS Flow Sheet for Property Model Validation**

The portion of the MAPPS PAT system relating to optical properties is summarized here. The first block (WOOD02) initializes both the flows of the stream components (fibers, water) and thermodynamic properties as well as performance attributes of fibers based in part on a species database. Previous pulping, bleaching, and refining operations are handled by overriding selected attributes with known values. For example, pulping yield, kappa number, and CS freeness are overridden with new values.

The light absorption at 457 nm is initialized in WOOD02 based on the weighted average of the specific absorptions of cellulose (3 cm<sup>2</sup>/g), lignin (338 cm<sup>2</sup>/g), and extractives (4 cm<sup>2</sup>/g), and the specific absorptions of any fillers which may be present.

$$K_{457} = \sum_{i=1}^4 K_i W_i \quad (18)$$

## Dye Mixing

The dye mixing block performs two simple functions. First the loadings of up to three dyes are specified. The model adjusts the mass flows of all the fiber components in the stream for mass balance assuming that all the dye is adsorbed uniformly on all fibers regardless of surface area or surface chemistry. These assumptions may be relaxed in future versions of the model. Next, the dye loadings are stored as PAT variables and passed to OPTPROP for optical property calculations.

## Optical Property Models

The performance attribute stream at a given point in the process is "passed" to the Optical Property block. The PAT variables in the performance attribute stream include pulp variables such as fiber composition, fiber length and width distribution, cell wall thickness, tensile and elastic properties of the fibers, specific surface areas, contact areas and bonding areas if a sheet has been formed, formation levels, stretch and fiber orientation, as well as suspended solids attributes and dye loadings.

The optical property block determines the properties of both a hypothetical handsheet made from the pulp with fiber attributes provided or a machine paper with network attributes provided. The key property needed to determine the optical properties is light scattering at 457 nm.  $K_{457}$  may also be provided directly by the user if it is known, thus overriding the value predicted by the WOOD02 block.

Additional data needed to determine handsheet scattering are handsheet pressing pressure, formation, stretch, and fiber orientation. For a Tappi handsheet, these are defaulted to 60 psi, 1.0 (ideal formation), 0% net stretch, and 45 degrees (random handsheet). Different estimates of these values must be provided to "simulate" a machine paper in the absence of a direct calculation with the paper machine models.

Figure 1 is appropriate for handsheet calculations but is highly simplified for predicting machine paper properties. For handsheets, Block 3 automatically calculates handsheet properties based on standard Tappi handsheet conditions. These may be overridden by

the user. However, for machine paper the performance attributes are determined by paper machine models to represent dewatering and densification on the wire and in the press nips, etc. In the absence of these models, pilot machine papers were simulated by specifying an effective pressing pressure to represent the pilot machine conditions. The optical property block then determined the densification which would take place in the forming and pressing operation and the light scattering coefficient of the base sheet. The final light scattering coefficient of the base sheet is the weighted average of the intrinsic scattering coefficients of the fibers in the bonded sheet and the average contribution of the suspended solids,

$$S_{sheet\ 457} = X_{susp} S_{susp} + (1 - X_{susp}) S_{fibers457} \quad (19)$$

where the scattering of the fiber network is given in terms of sheet density,  $\rho$ , adjusted for the average percent pulping yield,  $Y$ .

$$S_{fibers\ 457} = 50 + (24Y - 900)(1 - \rho) \quad (20)$$

Units are in  $\text{cm}^2/\text{g}$ . Sheet density is based on other models defined in terms of fiber contact area, cell wall thickness, fiber stiffness, yield and average specific surface area. If the predicted scattering is not sufficiently accurate, an experimental value can be entered to predict a more accurate K/S at 457 nm of the base sheet.

K/S of the base sheet at 457 nm is then determined from the separate K and S models or a value provided by the user. K/S at 16 equally spaced wavelengths is then determined using Eq. 17.

### Dye K/S data

The K/S data for each of three dyes are read in and stored in a database for use by the optical property blocks when needed. The data base was set up to read in one of several sets of dye data. The dye loadings are found from the performance attribute stream data. The mixture K/S is then determined over the visible range using Eq. 16 based on the base sheet K/S, the dye loadings, and the dye data.

$R_w$  is then determined from K-B theory (Eq. 12). Tristimulus values and  $L^*a^*b^*$  values are then determined from Eqs. 1 and 2 and 3 through 8, respectively. Sheet brightness and opacity are obtained by interpolating  $R_w$  between 450 and 460 nm and 570 and 580, respectively.

### Model Tuning

The scattering and absorption coefficients of the undyed stock were adjusted in the WOOD02 module to match the experimental data from the handsheet and paper machine

samples. In a more complete simulation model the pulp light absorption coefficient would be tuned through use of pulp composition data, particularly kappa number. The handsheet scattering coefficient would be one of several interrelated properties including density and tensile strength or elastic modulus which would be available to tune the predicted base sheet scattering coefficient. In a mill environment, fiber furnish data such as fiber length distribution and species information would also be available. The scattering coefficient of the machine paper would be the result of densification and bonding during paper forming, pressing, drying, and converting operations.

Nonideal dye retention could be simulated by reducing the dye loading on fibers parameters in the DYEMIX module. However, in the validation study, the dyes were assumed to be completely retained in the paper sheet.

## **MODEL VALIDATION**

A complete discussion of the results of this work may be found in Ref. 1. For the purposes of this discussion, only selected and representative data will be discussed here.

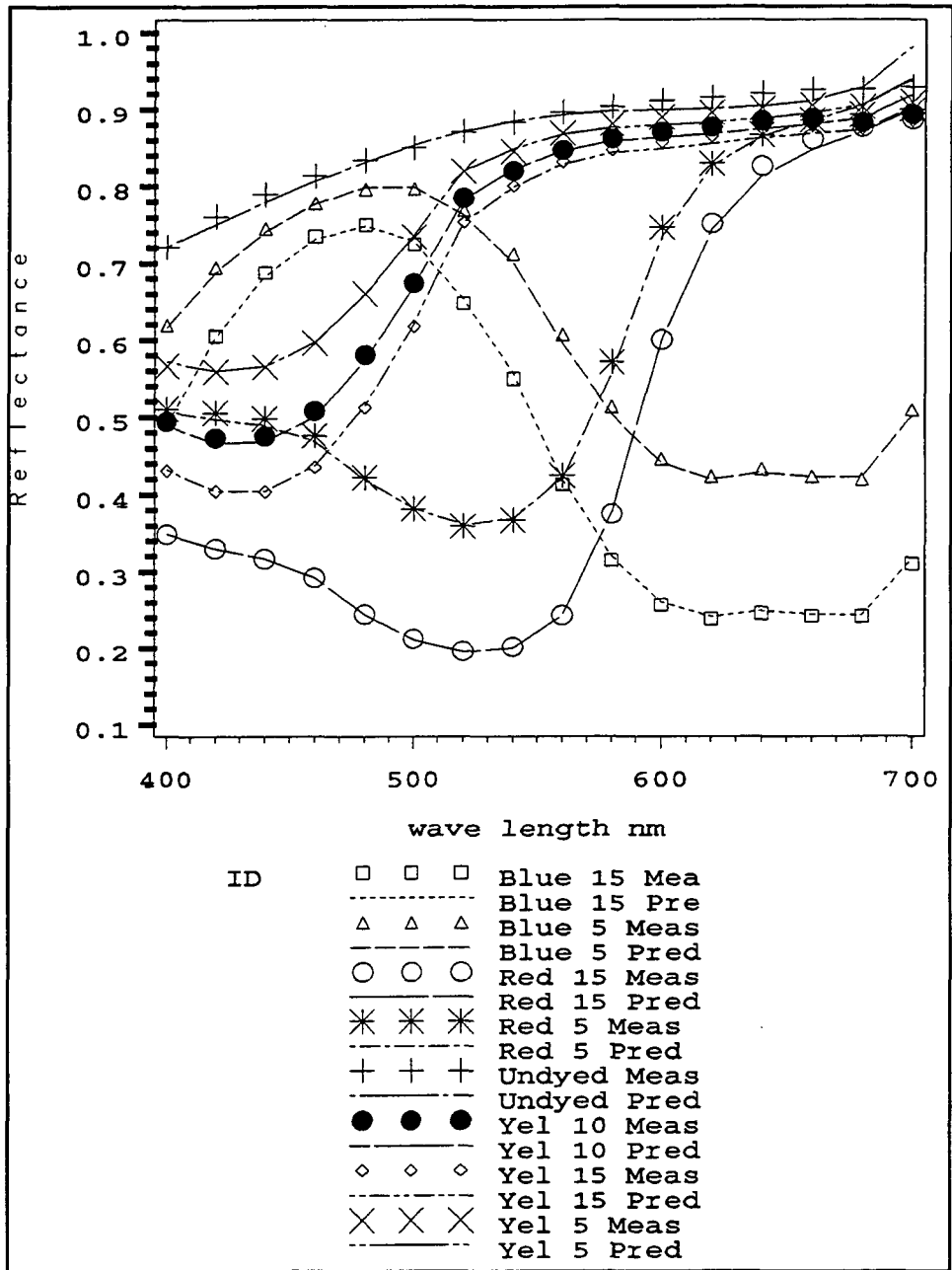
### **Reflectance of Calibration Paper**

Figure 2 shows the reflectance of the calibration handsheets for various dye loadings. Under the conditions investigated, the model accurately predicted the reflectance at all dye loadings.

The curves correspond to the following combinations of dyes: undyed; red, blue and yellow dyes at 5 and 15 lb/Am ton (0.25 and 0.75 wt. %); and additionally yellow at 10 lb/ton (0.5 wt. %). For the handsheets dyed with red dye, the maximum reflectance is in the range of 400 to 620 nm, while the maximum absorption is in the range of 400 to 620 nm, which is the red portion of the visible light spectrum. For the handsheets dyed with blue dye, the maximum reflection of light was in the wavelength range of 440 to 500 nm, giving the sheet its characteristic blue color. The maximum reflection of light for yellow-dyed handsheets was in the wavelength range of 520 to 700 nm. The maximum absorption of light was in the 400 to 520 nm wavelength range, resulting in the characteristic yellow color of the handsheets.

The change in the reflectance of the light is not linear with increasing concentration of dye in the sheet as can be predicted by Eq. 12. For this reason, the reflectance values were converted to the K/S values which show a linear relationship with increasing dye concentration from Eq. 16. The K/S coefficients of each dye can be found in the original reference (1, Tables 7 and 8).

With each pure dye, the reflectance curves in Fig. 2 are shifted downward as the loading increases. The effect of dye loading is accurately predicted, indicating that the linear mixing rule is justified.



**Figure 2 Effect of Pure Dyes on Reflectance-Calibration Handsheets**

## Color of Calibration Paper

The  $L^*a^*b^*$  values for various loadings of red dye are shown in Fig. 3. Again, the prediction of these values is very good over the entire loading range. The results are similar for the other individual dyes.  $L^*$  decreases, while  $a^*$  increases, and  $b^*$  remains relatively constant with increasing levels of red dye. The response is different for the blue and yellow dyes. Since  $a^*$  relates to redness-greenness, one would expect it to be sensitive to red dye.

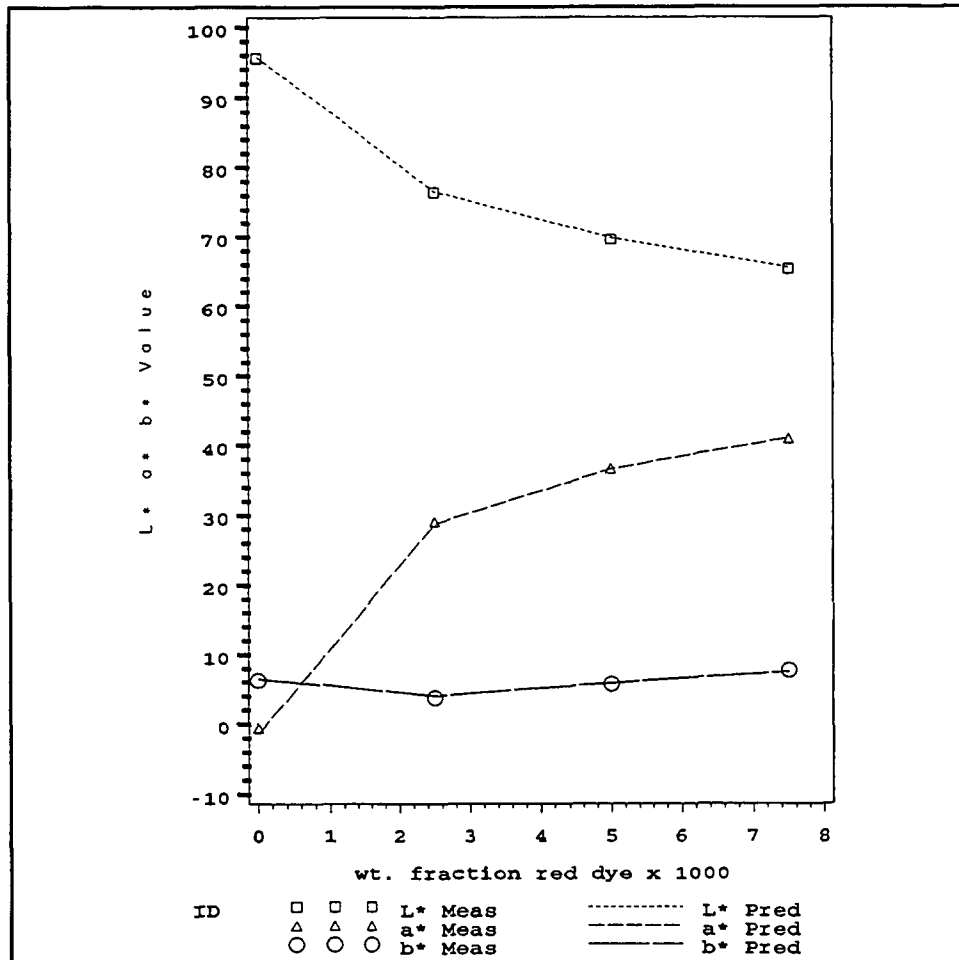


**Figure 3  $L^* a^* b^*$  Values for Calibration Handsheets-  
2 Degrees C Illuminant**

## Effect of Illuminant and Observer Angle

Figures 4 and 5 illustrate the effect of illuminant (C or D65) and observer angle (2 and 10 degrees) on the color difference,  $\Delta C$ . In all cases, as red dye loading increases, the color difference increases. These variables exert a subtle effect on color difference.  $\Delta C$  decreases in the following order: 2 deg D 65 > 2 deg C > 10 deg D 65 > 10 deg C. Figure 5 shows that the model predicts the effect of angle and illuminant quite accurately. For better visualization, the data are separated by 10 units.

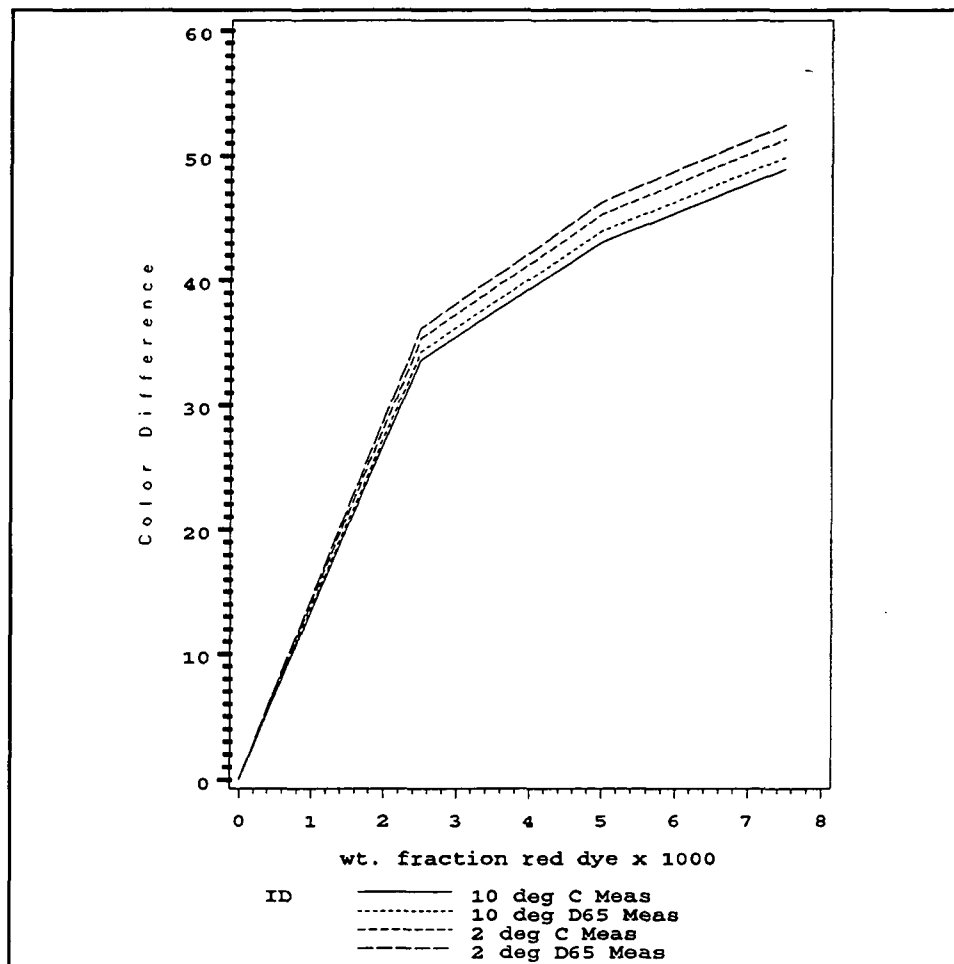
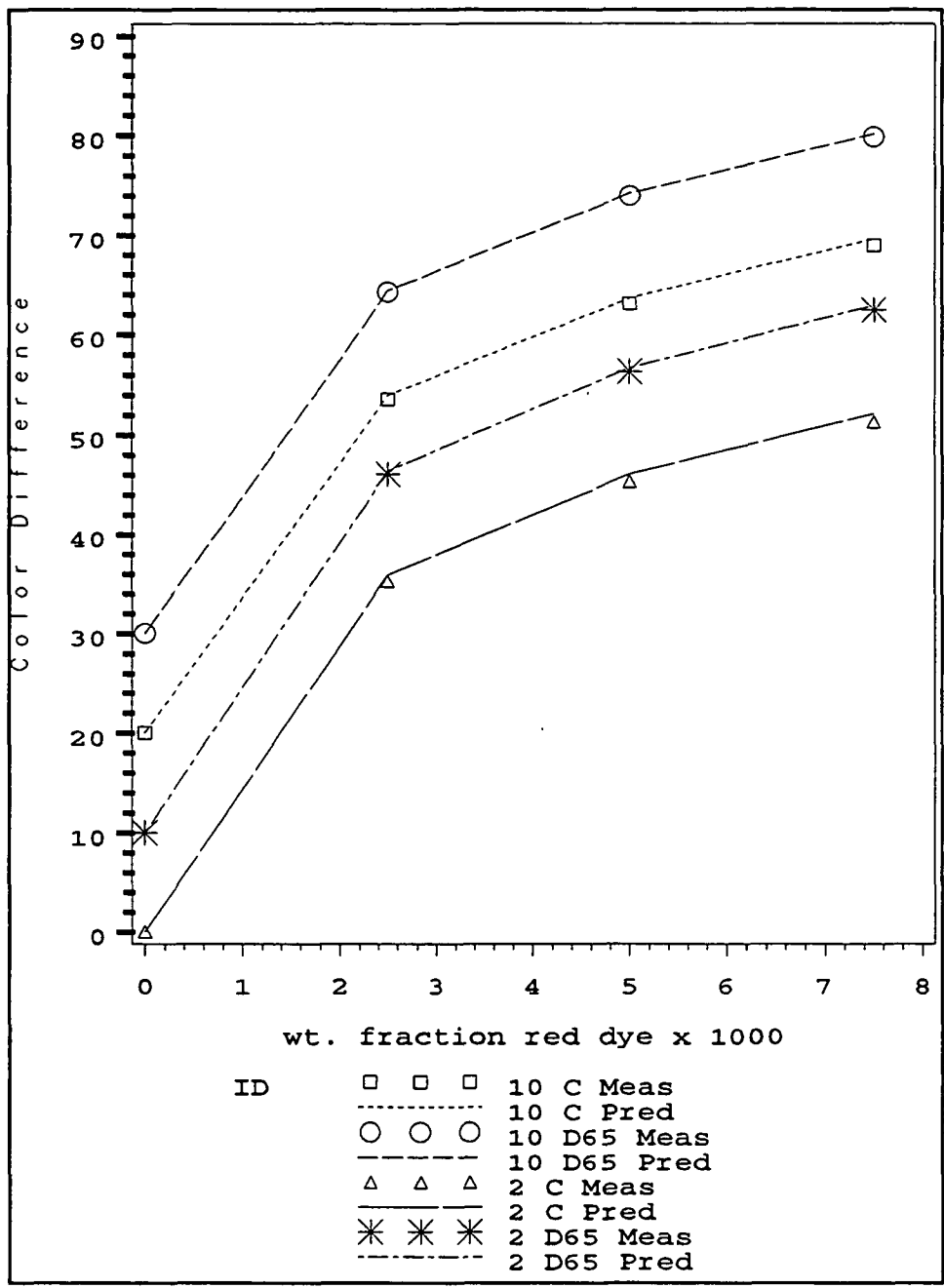


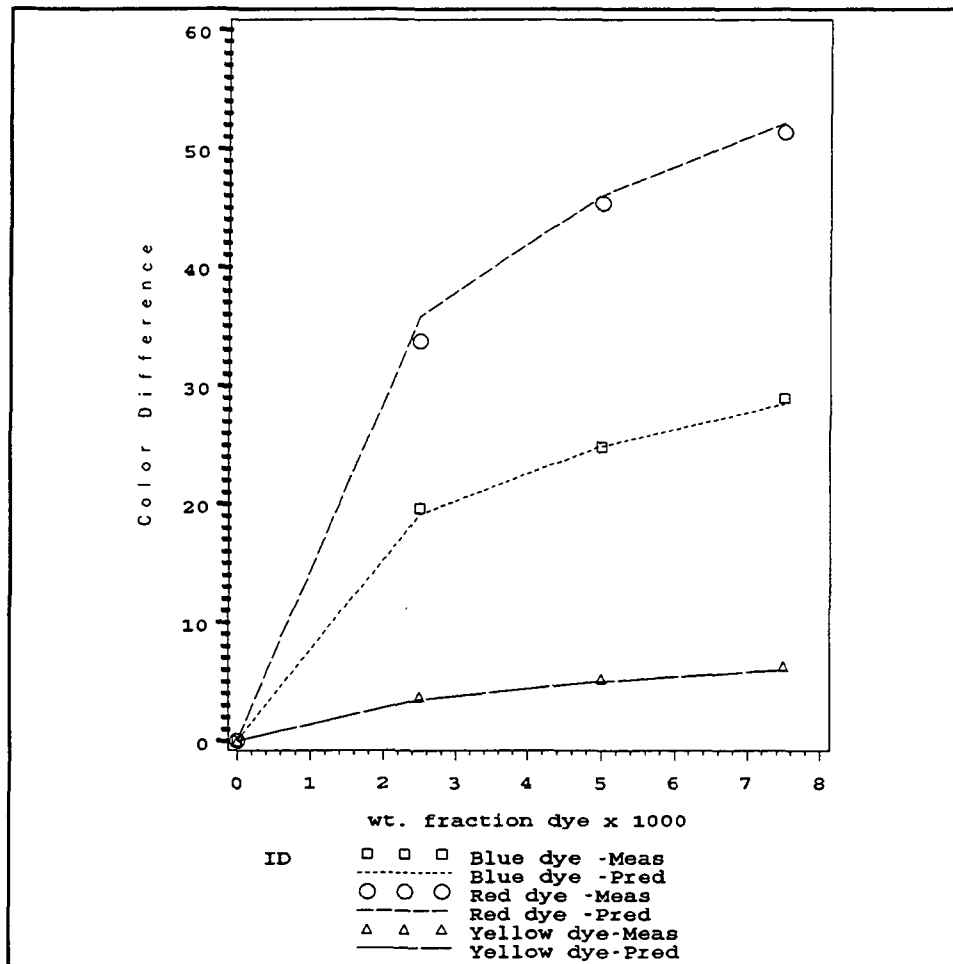
Figure 4 Effect of Observer Angle and Illuminant on Color Change-Calibration Handsheets



**Figure 5 Effect of Observer Angle and Illuminant on Color Change-Calibration Handsheets Measured and Predicted Values**

## Effect of Dye Loading on Color Difference

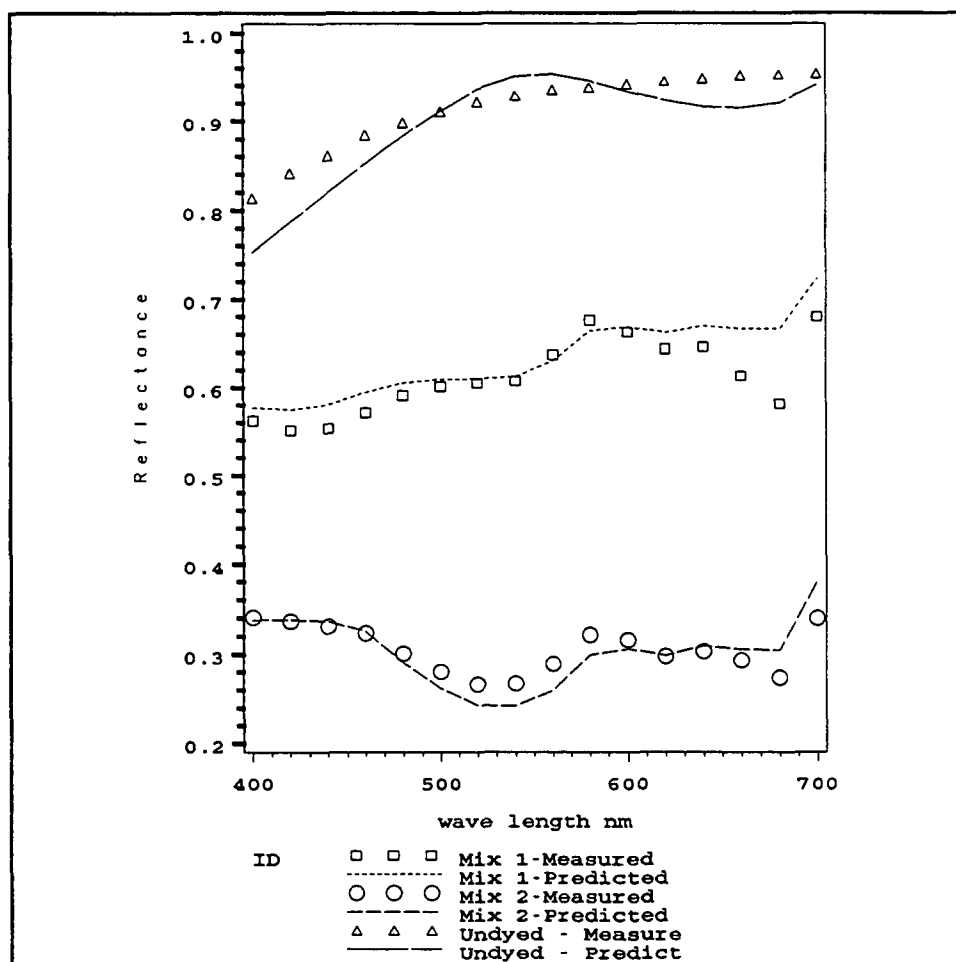
Figure 6 shows the effect of pure red, blue, and yellow dyes on color difference. Again, the model predictions are very accurate for all three dyes over the range in saturation. As expected, the color difference is greatest for red and least for yellow in qualitative agreement with our perception of these colors.



**Figure 6 Effect of Dye Loading on Color Difference-  
Calibration Handsheets  
Red, Blue, and Yellow Dyes**

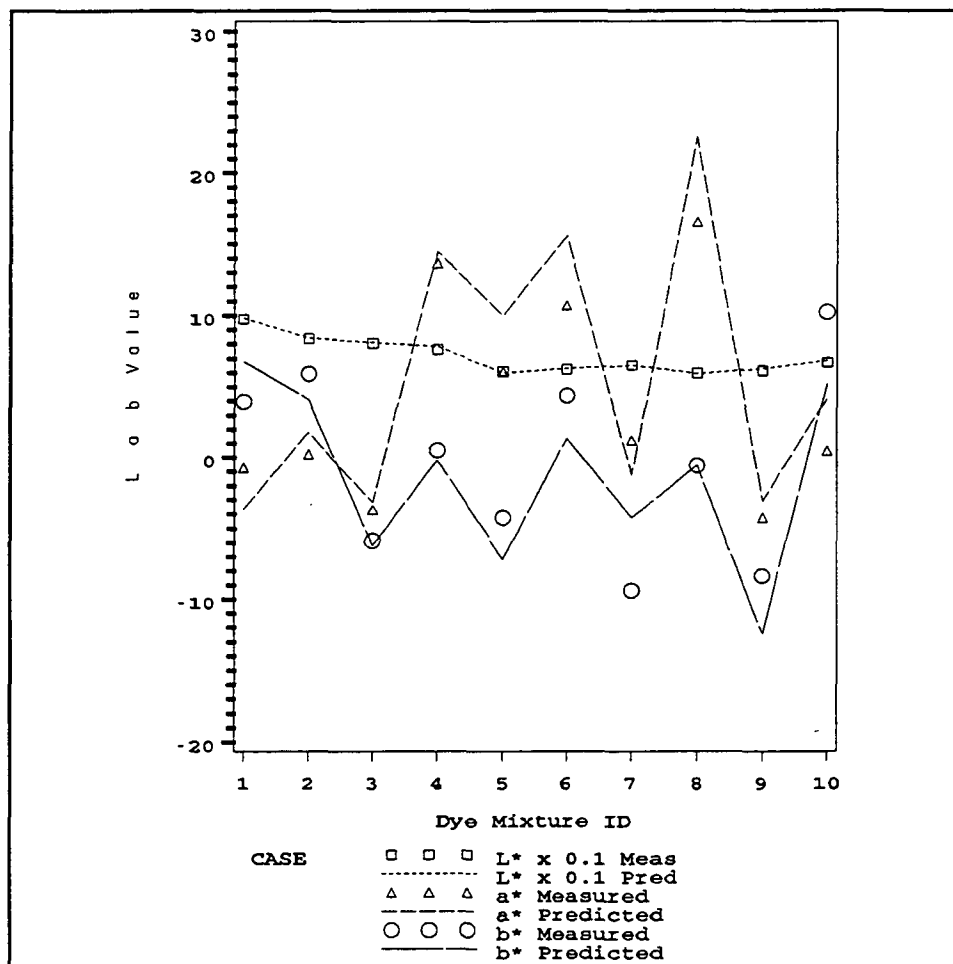
## Model Validation

Figure 7 shows the reflectance of pilot machine papers under three conditions: undyed - top curve, mixture 1 (.05, .05, and .15 wt. %, red, blue, and yellow respectively), middle curve and mixture 2 (.5, .5, and .25 wt % red, blue, and yellow), lower curve. The largest errors occur in the undyed sheet, and these are reflected in the deviations at the higher dye loadings for the mixtures. The deviations between the measured and predicted reflectance of the undyed sheets for the validation papers (machine, handsheets, and couch handsheets) led to similar differences in the predicted  $L^*a^*b^*$  values. Figure 7 shows that reflectance decreases with increasing dye mixture loading.



**Figure 7 Effect of Dye Mixtures on Reflectance of Machine Paper**

The effect on  $L^*a^*b^*$  of dye mixtures is shown in Fig. 8.  $L^*$  values decrease generally with increased dye loading from left to right, while  $a^*$  and  $b^*$  values are much more sensitive to the combinations of dyes.  $a^*$  is sensitive to red, while  $b^*$  is most sensitive to blue. Again, the model predictions are quite good. The variations in  $a^*$  and  $b^*$  for each combination of dyes are accurately determined by the model, although the absolute value of the change may not always be predicted exactly.



**Figure 8 Effect of Dye Mixtures on  $L^* a^* b^*$  Values-  
Machine Papers  
Red, Blue, and Yellow Dyes**

## Color Change

As pointed out previously, the error in the  $L^*a^*b^*$  values comes about because of the error in the undyed base sheet reflectance curves. When the color differences relative to the undyed sheet are compared for the same set of dye mixtures, the agreement is remarkably good as shown in Fig. 9. The color difference increases with increased dye loading as observed earlier with the calibration handsheets. To better visualize each curve, the values were offset by 10 units. Generally, the response of each type of handsheet is similar for each dye mixture, although this is not always the case. For example, mixtures 5 and 7 show differences between the validation handsheets and the couch or machine papers. The model very accurately predicts the effect of dyes on each type of sheet after correcting the undyed values.

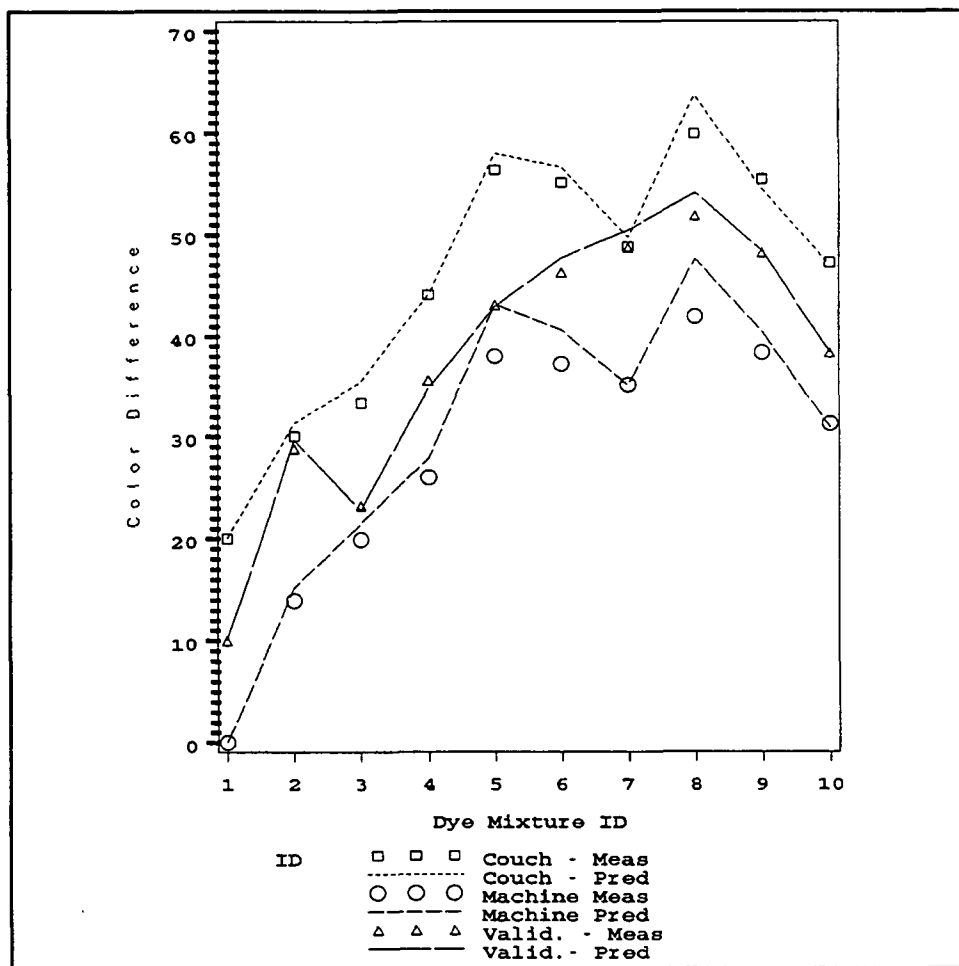


**Figure 9 Effect of Dye Mixtures on Color Change  
Machine Papers, Validation and Couch Handsheets  
Red, Blue, and Yellow Dyes**

## Lab Values for the Validation Papers

The Lab values for the dye mixtures for the validation handsheets are shown in Fig. 10. For clarity, the  $L^*$  values have been divided by 10. Correspondence between Dye Mixture ID and dye loadings can be found in Table 2. Again, the agreement is remarkably good. The observations made previously for the behavior of Lab for the machine papers also apply to the couch handsheets. However, the agreement for  $a^*$  and  $b^*$  is generally better than that for the machine papers.

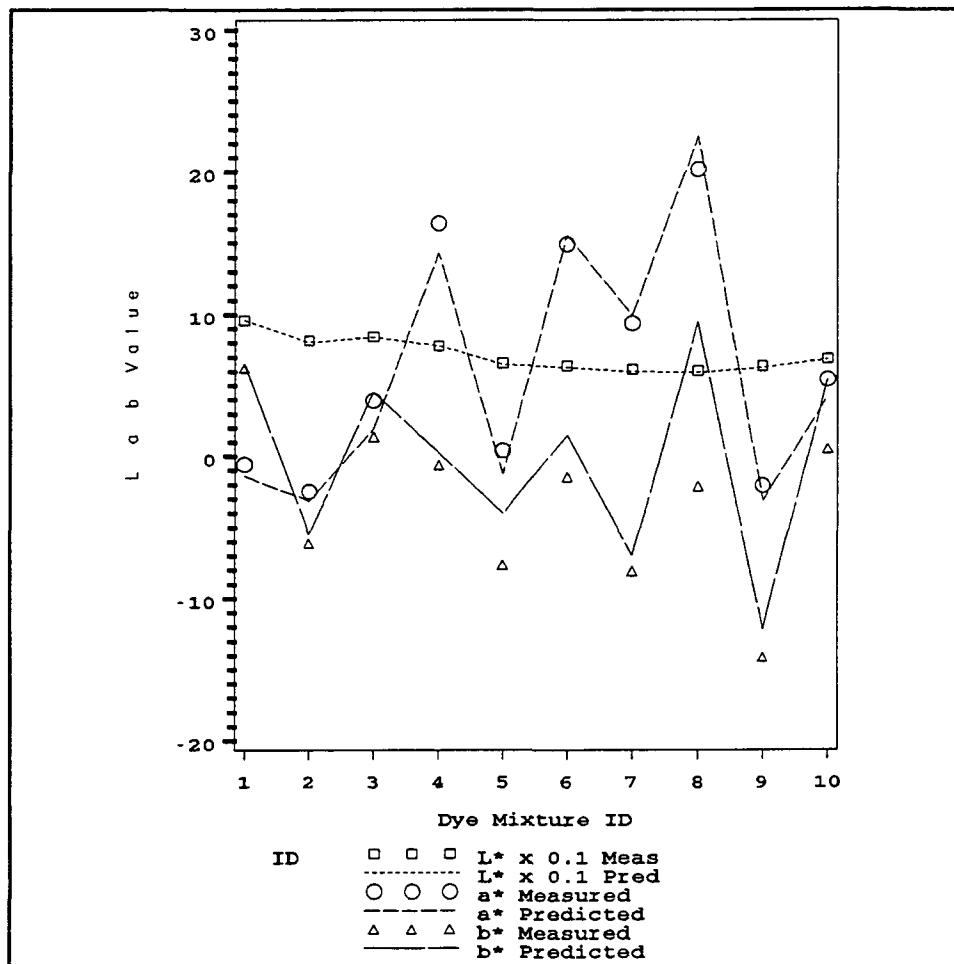


**Figure 10 Effect of Dye Mixtures on  $L^*$   $a^*$   $b^*$  Values-  
Validation Handsheets  
Red, Blue and Yellow Dyes**

## Tinted Sheets

The L\*a\*b\* values for tinted handsheets for the undyed sheet and dye mixture cases are shown in Fig. 12. The correspondence between the Dye Mixture ID and dye loadings can be found in Table 3.

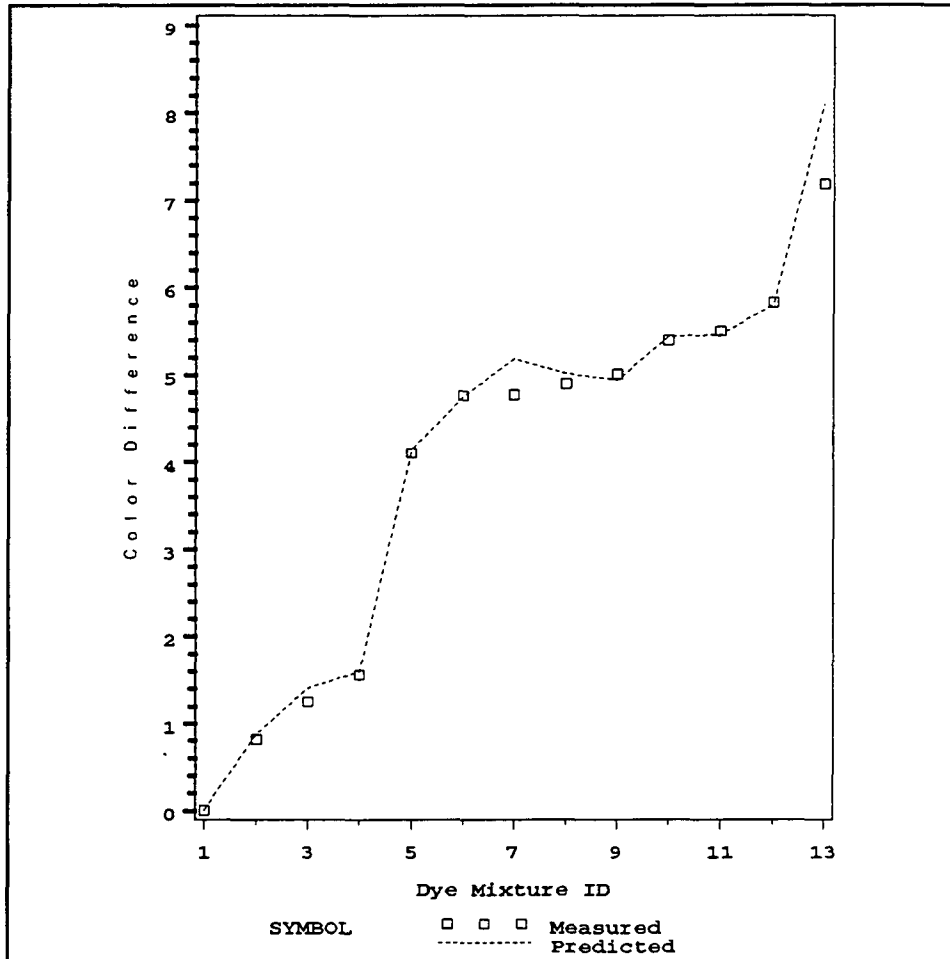


**Figure 12 Effect of Tints on Color Change-  
Combined Calibration and Validation Handsheets  
Mixtures of Red, Blue, and Black Dyes**

The color difference response to dye mixtures at tinted conditions is accurately predicted as shown in Fig. 13. The absolute color difference is, of course, much smaller due to the lower levels of dye used. The dye mixtures were not applied in the order shown. Instead, the mixtures were sorted in generally increasing saturation for presentation purposes.

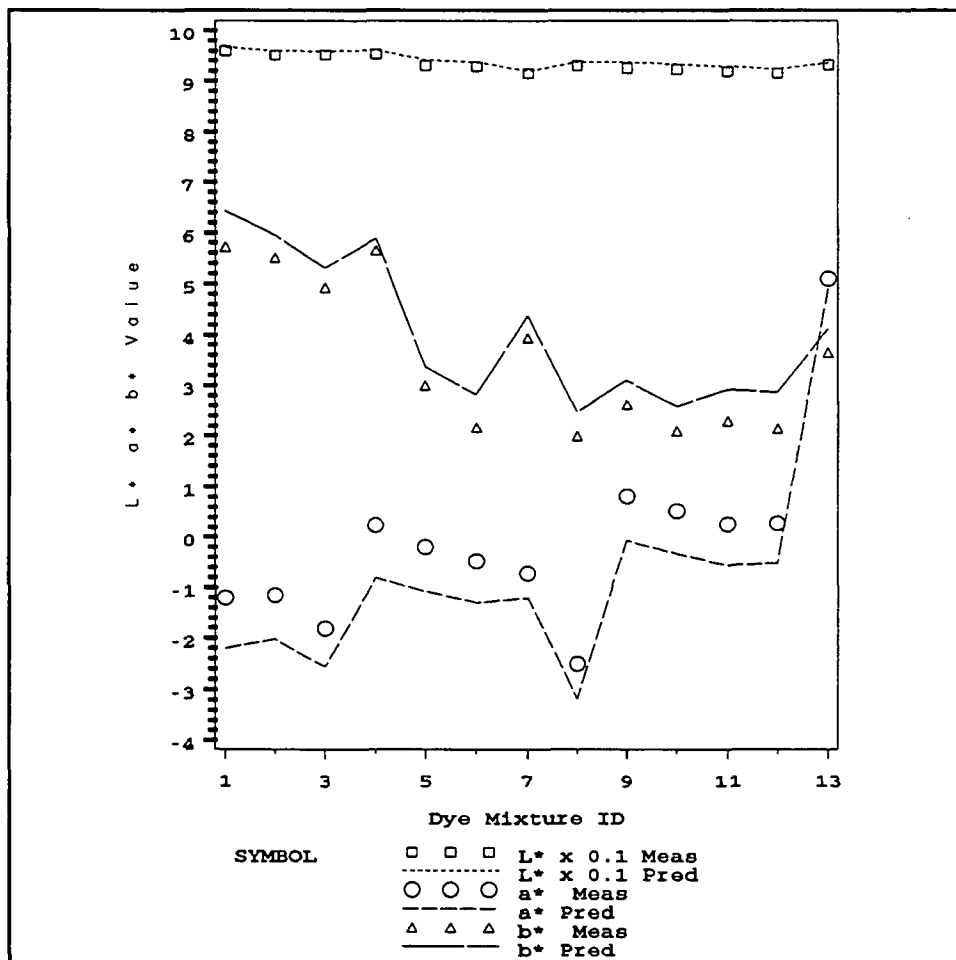


**Figure 13 Effect of Tints on L\* a\* b\* Values-  
Combined Calibration and Validation Handsheets  
Mixtures of Red, Blue, and Black Dyes**

## CONCLUSIONS AND RECOMMENDATIONS

It is evident from the analysis that the models developed in this study are capable of predicting the optical properties of the handsheets as well as machine paper. The errors in the color coordinate values are due primarily to the reflectance curve of the undyed sheet. Therefore, given methods to more accurately predict the behavior of the undyed sheet, the system will accurately predict absolute color coordinates. The system can also predict changes in color quite accurately.

The effects of dye loadings, observer angle and illuminant type are also accurately predicted. This level of agreement indicates that the original assumptions of uniform loading and full saturation of the dyes were correct. Other assumptions particularly those regarding the applicability of linear mixing theory and Kubelka-Munk theory are also valid.

The system could be readily used for any combination or type of cationic dyes (not fluorescent dyes) by substituting the dye reflectance values into the system database. It is conceivable that the simulation system could form a part of an on-line control system to automatically adjust the addition of dyes in the papermaking system to control the final dry color of the sheet. This would constitute a significant application of paper physics principles and simulation technology in the improvement of optical quality of fine paper.

Mixture I.D.	Dye Loading wt. fraction x 1000		
	Red	Blue	Yellow
1	0	0	0
2	0.5	0.5	1.5
3	1.5	0.5	0.5
4	0.5	1.5	0.5
5	5.0	5.0	2.5
6	2.5	5.0	5.0
7	5.0	2.5	5.0
8	2.5	7.5	2.5
9	7.5	2.5	2.5
10	2.5	2.5	7.5

Table 2. Dye Mixture Combinations for Saturated Validation Papers

Mixture I.D.	Dye Loading wt. fraction x 10 <sup>5</sup>		
	Blue	Red	Black
1	0	0	0
2	0	0	1.56
3	1.56	0	0
4	0	0.78	0
5	0	1.41	0
6	4.23	1.41	0
7	5.63	0	0
8	0	0	15.63
9	7.81	2.34	0
10	1.09	2.34	0
11	5.62	1.88	0
12	4.69	1.88	5.63
13	0	6.25	0

Table. 3 Dye Mixture Combinations for Tinted Papers

## REFERENCES

1. Chaturvedi, Mayunk, "Prediction of Paper Color - A Process Simulation Approach," M.S. Thesis, Western Michigan University, (1992).
2. Johnston, R.M., "What is Color?," Symposium on Industrial Color Technology, American Chemical Society, September (1968), 4-16.
3. Hunt, R.W.G., **Measuring Colour**, 1st. edition, John Wiley and Sons, New York, (1987), 105-113.
4. Judd, D.B. and Wyszecki, G., **Color in Business, Science, and Industry**, 3rd edition, John Wiley and Sons, New York, (1975), 125-139.

5. McLaren, K., **The Color Science of Dyes and Pigments**, 2nd edition, Hilger, Bristol, (1986), 101-102.
6. McLaren, K., **The Color Science of Dyes and Pigments**, 2nd edition, Hilger, Bristol, (1986), 126-127.
7. *ibid.* Hunt, R.W.G., 117-118.
8. Billmeyer, Jr., F.W. and Richards, L.W., "Scattering and Absorption of Radiation by Lighting Materials," **Journal of Color and Appearance**, 11(2) Summer, (1973), 4-15.
9. Klier, K., "Absorption and Scattering in Plane Parallel Turbid Media," **Journal of the Optical Society of America**, 62(7), (1972), 882-885.
10. Mudgett, P.S. and Richards, L.W., "Multiple Scattering Calculations for Technology," **Applied Optics**, 10(7), (1971), 1485-1502.
11. Kuehni, R.G., **Computer Colorant Formulation**, 1st edition, D.C. Heath, Lexington, (1975), 13-15.
12. *ibid.*, 27-29.
13. Van den Akker, J.A., **Optical Properties of Paper**, **Handbook of Paper Science** (ed. H.E. Rance), Elsevier, NY, 2, (1982), 168-171.
14. Steele, F.A., "The Optical Characteristics of Paper," **Paper Trade Journal**, 100(12), (1935), 37-42.
15. *ibid.* Kuehni, R.G. 25-27.
16. Nolan, P., "The Calculation of the Spectral Reflectivity of Dyed Handsheets," **Paper Trade Journal**, 105(14), (1937), 37-42.
17. Herbst, J.H.E. and Kraessig, H., "Determination of Optical Properties of Pulp," **Tappi**, 43(10), (1960), 836-839.
18. Lange, P. W. and Lindvall, E., "Adsorption and Diffusion of Substantive Dyes in Cellulose Fibers," **Svensk Papperstid.** 57(7):235-241 (1954).
19. Thode, E.F. et al., "Dye Adsorption on Wood Pulp. II," **Tappi**, 35(8), (1952), 379-384.
20. Thode, E.F. et. al., "Dye Adsorption on Wood Pulp. III," **Tappi**, 36(11), (1953), 498-504.

21. MAPPS (Modular Analysis of Pulp and Paper Systems) Technical Documentation, Copyright, Institute of Paper Science and Technology (1993).
22. Jones, G.L., "New Directions in Process Simulation," Proceedings 21st Annual PIMA/MIS International Conference, p. 377 (1989).
23. Jones, G.L., "Simulating the Development of Pulp and Paper Properties in Mechanical Pulping Systems," **Pulp and Paper Canada**, 89(6), (1988), 128-138.
24. Jones, G.L., "Simulating End-Use Performance," **Tappi**, 90(10), (1989), 189-197.
25. Jones, G.L., "Simulation of the Performance Characteristics of a TMP Mill," **Pulp and Paper Canada**, 91(2):69-76, (1990).
26. Jones, G.L. and Nguyen, X., "Analysis and Simulation of Property Development in Forming Newsprint," **Tappi** 73(7):160-168 (1990).